Electrochemical and Solid-State Letters, **8** (9) A464-A466 (2005)
1099-0062/2005/8(9)/A464/3/$7.00 © The Electrochemical Society, Inc.

Tin Nanoparticles Formed in the Presence of Cellulose Fibers Exhibit Excellent Electrochemical Performance as Anode Materials in Lithium-Ion Batteries

Álvaro Caballero, Julián Morales,* and Luis Sánchez[z]

Departamento de Química Inorgánica e Ingeniería Química, Facultad de Ciencias, Campus de Rabanales, Edificio Marie Curie, Universidad de Córdoba, 14071 Córdoba, Spain

A one-step chemical reduction procedure affords the effective preparation of highly crystalline and disperse tin nanoparticles by virtue of the presence of cellulose fibers. These fibers play a crucial role as particles grow on their surface, which prevents agglomeration. The Li/Sn-cellulose cell exhibits very good electrochemical performance which makes the composite an excellent electrode material for lithium cells.
 [DOI: 10.1149/1.1993388]

Manuscript submitted March 21, 2005; revised manuscript received May 30, 2005. Available electronically July 18, 2005.

The need for higher energy Li-ion battery electrode materials has driven research on both cathode and anode materials.[1,2] Research into anode materials has focused on elements such as Sn, Si, and Sb, which alloy reversibly with Li and possess higher gravimetric and volumetric capacities than do graphite materials commonly used in current commercial Li-ion batteries. Tin reacts with lithium[3] to form various Li_xSn type compounds that can provide a theoretical capacity of 993 Ah kg^{-1}. When used alone as an anode material, however, this metal loses capacity rapidly as a result of the large volume change associated with the formation of various Li-Sn phases. Thus, Li_xSn goes through five different crystallographic phases over the range $0 < x < 4.4$ involving volume changes as large as 260%.[4] The concurrence of phases with different Li concentrations leads to nonhomogeneous volume expansions. Cracking of alloy grains results in poor conductivity due to the loss of electrical contact, which detracts from long-term cycling performance.[5]

Reducing the particle size of the Li^+ storage material or the extent of alloying are believed to improve performance. Thus, Whitehead et al.[6] have shown that using smaller particles of Sn increases reversibility. Also Li et al.[7] used a sol-gel template synthesis method to prepare thin films of SnO_2 nanofibers that exhibited very high capacity and increased capacity retention even at high discharge rates. Likewise, amorphous Sn-based materials have been found to exhibit an improved cycling behavior.[8] On the other hand, SnO_2 and Sn-based nanoparticles used as anode materials undergo an irreversible capacity loss through decomposition of tin compounds in the first lithiation cycle ($SnO_2 + 4Li^+ \rightarrow Sn + 2Li_2O$).[9] As a remedy, Besenhard et al.[10] suggested the incorporation of nanosized active alloying species such as Sn into an inactive matrix to suppress Li-Sn phase transitions. Thus, the inactive matrix disperses the Li_xSn aggregates and buffers the volumen expansion caused by the alloy formation, hindering the formation of cracks in the electrode during the lithium insertion process. In this respect, SnSb,[11] Sn_2Fe-$SnFe_3C$[12] and Cu_6Sn_5[13] systems exhibit an improved cycling behavior; however, their experimental capacity is much lower than the theroretical values for Sn, usually, as a consecuence of the matrix being electrochemically inactive.

The most effective way of developing high-capacity tin-based anodes may be by preparing Sn particles of a small size (particularly on the nanoscale). Particles thus obtained must be stabilized to avoid agglomeration during use and hence the loss of their advantages. In this respect, carbonaceous materials have recently been used as matrices to disperse Sn nanoparticles with the aim of combining the good cyclability of the carbon host and the high capacity of tin.[14-16] However, the capacity of carbon-tin composites is generally between those of their constituents (450–200 Ah kg^{-1}) because the carbonaceous host can only accommodate small amounts of tin (30–15% or less); also, the operational potential range is expanded (0.0–2.0 V).

Preparing nanosized Sn particles is difficult and has only been accomplished in a few cases. Nayral et al. obtained 15–25 nm tin particles by thermolysis of $[Sn(NMe_2)_2]_2$.[17] Physical vapor deposition-based techniques, while relatively more common, are expensive as an alternative to the chemical preparation of nanoscale Sn.[18] Although the direct chemical reduction of tin salts often produces particles larger than 1 μm, nanosized particles can be obtained using surfactant or chelating agents, and also by thermal decomposition of inorganic or organic precursors in a reductive atmosphere.[15,16,19]

This paper reports a one-step method for the preparation of Sn nanoparticles simply by chemical reduction of $SnCl_4$ with KBH_4 at ambient temperature for a short time, using cellulose as physical spacer. Other than the insertion of tin into carbon nanotubes, which occurs to a very small extent,[20] this is the first time nanometric tin particles have been obtained in the presence of sorbent fibers in the precursor solution rather than by using foreign species such as surfactant or chelating agents. Although cellulose fibers are difficult to remove, this poses no problem here as the cellulose-tin system constitutes an advanced, fully operational electrode as shown below.

Experimental

All chemicals used in this work were analytical grade. Tin nanoparticles were synthesized as follows. 200 mg of celullose fibers (Arbocel) was added to a solution containing 1.0 g of $SnCl_4 \cdot 5H_2O$ dissolved in 2 mL H_2O under continuous stirring for 30 min to ensure thorough soaking of the fibers. Then, 3.0 mL of 4 M KBH_4 was added dropwise, the cellulose fibers rapidly acquiring a grey color. After stirring for 10 min, the emulsion was filtered and washed with distilled water and ethanol several times. For avoiding the composite to be in contact with air, it was soaked with ethanol prior to drying in a vacuum oven at 60°C for 3 h.

X-ray powder diffraction (XRD) patterns were recorded on a Siemens D5000 X-ray diffractometer, using Cu Kα radiation and a graphite monochromator. Scanning electron microscopy (SEM) and high-resolution transmission electron microscopy (HRTEM) images were obtained with a JEOL 6400 and a JEOL 2010 microscope, respectively. Electrochemical measurements were performed in two electrode Swagelok-type cells, using lithium as a counter electrode. The electrolyte was Merck battery electrolyte LP 40 (EC:DEC = 1:1 w/w, 1 M $LiPF_6$). Electrode pellets were prepared by pressing, in a stainless steel grid, ca. 2 mg of synthesized composite. Galvanostatic tests were conducted under C/4 galvanostatic regime (C being defined as 1 Li^+ exchanged in 1 h). All electrochemical measurements were controlled via a MacPile II potentiostat-galvanostat.

* Electrochemical Society Active Member.
[z] E-mail: luis-sanchez@uco.es

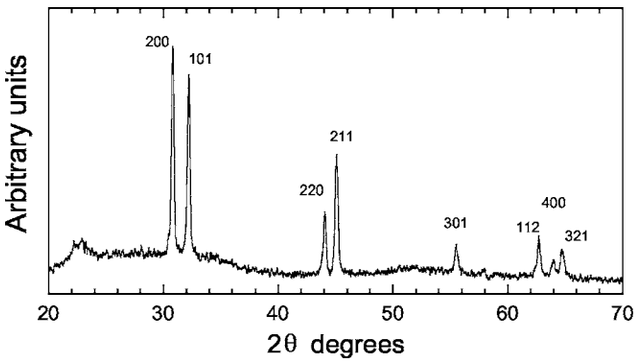

Figure 1. XRD patterns for the Sn-cellulose composite.

Results and Discussion

Figure 1 shows the XRD pattern for the tin-cellulose fiber system. The first broad peak, at 23° 2θ, corresponds to the cellulose component; all others can be indexed to a tetragonal cell with $a = 0.582$ and $c = 0.317$ nm, all of which are consistent with the values for tetragonal Sn. Also, the relative intensity of peaks is consistent with that reported elsewhere.[21] The Sn-containing sample consisted of cross-linked cellulose fibers covered by tin particles. Figure 2 shows selected electron microscopy images of isolated cellulose fibers before and after deposition of Sn; note their sharp, well-defined boundaries (Fig. 2A). Upon reduction, however, the fibers exhibited a wrinkled surface (Fig. 2B) suggesting that they were coated by tin particles. The natural tendency of Sn nanoparticles to form agglomerates was hindered by the presence of the cellulose fibers. Also, the additive facilitated the formation of flake-shaped nanoparticles in sizes from 20 to 30 nm (inset Fig. 2B), probably as a result of fiber surfaces acting as nucleation sites for Sn particles. In fact, in the absence of cellulose, the chemical reduction of $SnCl_4$ led to Sn particles 2–4 μm in size (i.e., two orders of magnitude greater than those in Fig. 2). Figure 3 shows HRTEM images of a tin nanoparticle. The lattice fringes reflect the crystalline nature of the Sn nanoparticles. The interplanar spacing is about 0.296 nm, corresponding to the orientation of (200) atomic planes of tetragonal Sn. Lattice fringes of a different orientation were also observed that were more pronounced at particles boundaries and suggest some structural disorder. The amount of tin deposited onto the fibers was calculated by calcining the composite in the air at 850°C for 4 h; under these conditions, only a 6% by weight corresponds to carbon from pyrolysed cellulose and Sn was oxidized to SnO_2. The calculated Sn content was 29.4%.

The electrochemical response of the sample thus prepared was measured in a two-electrode $Li/LiPF_6$ EC-DEC/Sn-cellulose cell. The working electrode contained no electronic conductor or binder additives such as carbon black or PTFE. The open-circuit potential of the cell was 2.6 V (a typical value for Li/Sn cells). During the first discharge (Fig. 4), the potential dropped abruptly to a broad plateau at 0.25 V. No potential plateau was observed in the 1.1–0.9 V region, which is typical of the reduction of SnO_x species. All lithium taken up must be inserted into Sn nanoparticles as cell made from pure cellulose delivered a negligible capacity. However, the faradaic yield considerably exceeded that required for the high-content lithium alloy $Li_{4.4}Sn$ to form. This suggests the presence of competitive reactions such as electrolyte reduction at potentials below 0.5 V. Species such as $(CH_2OCO_2Li)_2$ and $C_2H_5OCO_2Li$ are believed to be formed by reduction of EC and DEC solvent when a Li/SnO cell is discharged below 0.7 V.[22] This process may be catalyzed by the nanosized tin flakes and accounts for the high irreversible capacity obtained in the first discharge curve. Subsequent charge-discharge curves for the cell cycled over the 1.0–0.0 V range exhibited the typical shape for Li/Sn based cells and were consistent

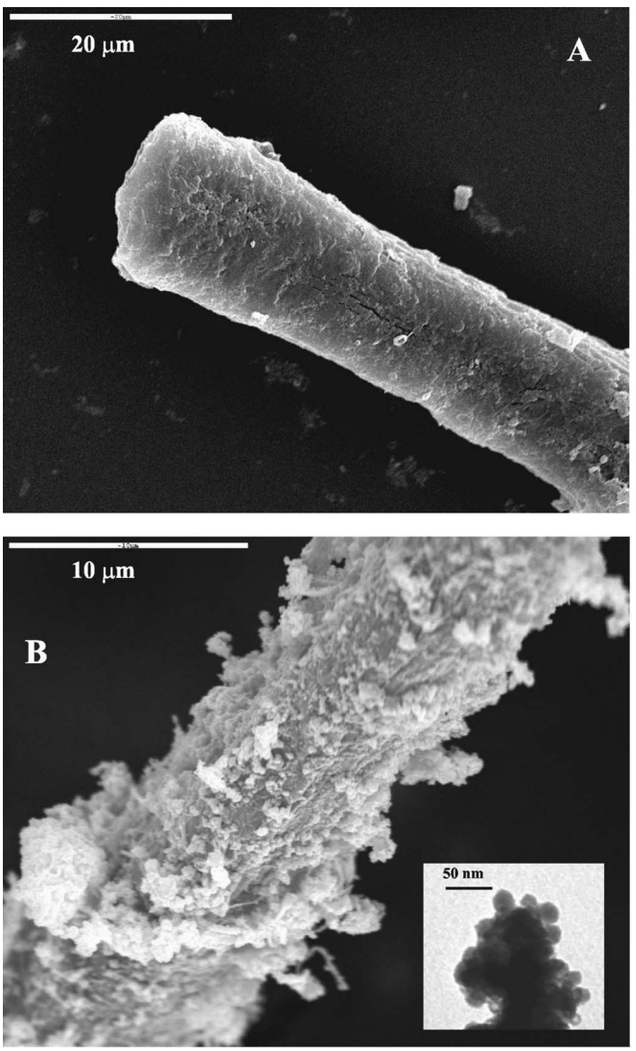

Figure 2. SEMs of cellulose fibers (A) before and (B) after the reduction process. The inset shows a TEM image obtained from tin particles at the fiber border.

with the reversible reaction $Sn \Leftrightarrow Li_xSn$. Note the increase in cell capacity over the first few cycles. After the fifth cycle, however, the capacity virtually leveled off.

Figure 5 shows the variation of the specific capacity of the $Li/LiPF_6$ EC-DEC/Sn-cellulose cell with the number of cycles. Capacity retention was excellent and an average value of 607 Ah/kg (this value is calculated by mass of tin; the capacity decreases to 140 Ah/kg referred to total weight of Sn plus cellulose) was maintained on extended cycling. Also, from the tenth cycle the charge recovery, a term that defines the specific capacity stored by the cell in the charge process in relation to that delivered in the previous discharge process, is virtually 100%, indicative of the reversibility of the Li/Sn system.

To our knowledge, no reported Li/Sn cell has the ability to retain such high capacity values and only a few tin-based oxides and alloys with a similar or slightly higher capacity exist; however, they involve more complex synthetic and electrode preparation procedures.[7,23-25] Such an outstanding electrochemical behavior can be ascribed to the presence of cellulose during the synthesis, which results in well-dispersed nanosized tin particles, and also to the electrode composition. Thus, the volume expansion occurring during the formation of Li_xSn alloys is easily absorbed by the fibers, which

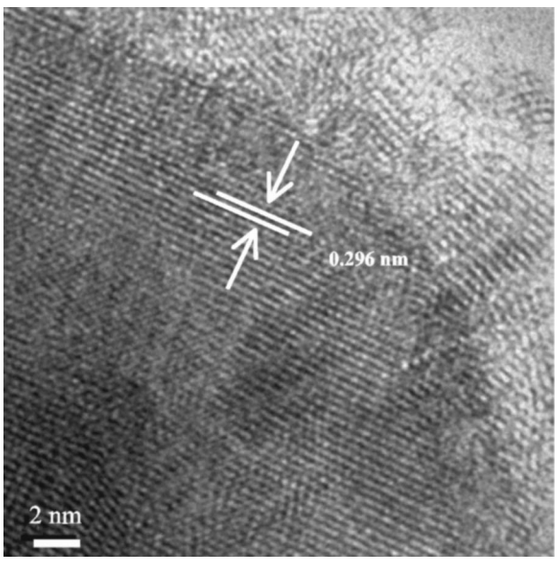

Figure 3. HRTEM images of Sn nanoparticles.

therefore minimize cracking between alloyed particles. The particles are always in contact with enough charge carriers to preserve the reversibility of the electrochemical process. On the other hand, if the tin particles are prepared via chemical reduction in the absence of cellullose and then both components are manually mixed, the resulting electrode exhibits very poor capacity retention (open circles in Fig. 5). The poor performance of this cell may be a result of *(i)* the increased size of Sn particles (2–4 μm) and *(ii)* inefficient particle dispersion despite the presence cellulose fibers, the buffering effect on volume changes during the alloying process is suppressed. The resulting micrometric particles crack during the alloying process, which reduces electrical contact and hence cell capacity.

In summary, the proposed simple, one-step chemical reduction procedure affords the effective preparation of highly crystalline and disperse tin nanoparticles by virtue of to the presence of cellulose fibers; the fibers play a crucial role: as particles grow on their surface, which prevents agglomeration. These properties make the composite an excellent electrode material for lithium cells as it exhibits very good electrochemical performance, without the need for any additives. The Li/$LiPF_6$ EC-DEC/Sn-cellulose cell delivers capacities above 600 Ah kg^{-1} on prolonged cycling. This preparation method can be extended to other systems of potential interest as electrode material for Li-ion batteries.

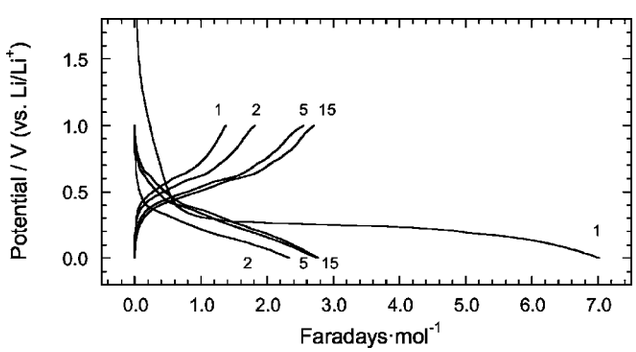

Figure 4. First galvanostatic discharge/charges curves recorded at C/4.

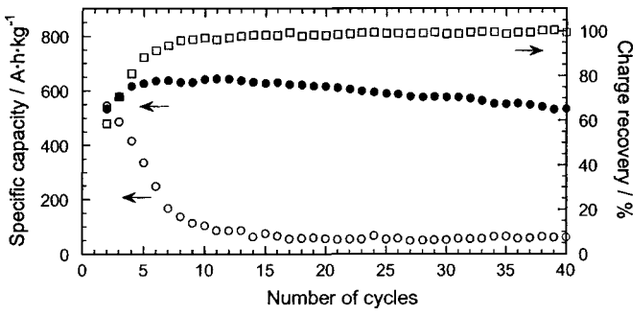

Figure 5. Specific discharge capacity (●) and charge recovery (□) for the Li/Sn-cellulose cell as a function of number of cycles. Specific discharge capacity (○) delivered by the electrode made from tin and cellulose mixed manually.

Acknowledgment

This work was funded by Junta de Andalucía (Group FQM-175) and Spain's Ministry of Science and Technology (project MAT2002-04477-C02-02).

Universidad de Córdoba assisted in meeting the publication costs of this article.

References

1. C. R. Sides and C. R. Martin, *Adv. Mater. (Weinheim, Ger.)*, **17**, 125 (2005).
2. H. Li, G. Ritcher, and J. Maier, *Adv. Mater. (Weinheim, Ger.)*, **15**, 736 (2003).
3. J. Wang, I. D. Raistrick, and R. A. Huggins, *J. Electrochem. Soc.*, **133**, 457 (1986).
4. L. Y. Beaulieu, K. W. Eberman, R. L. Turner, L. J. Krause, and J. R. Dahn, *Electrochem. Solid-State Lett.*, **4**, A137 (2001).
5. R. A. Huggins, in *Handbook of Battery Materials*, J. O. Besenbard, Editor, Wiley-VCH, Weinheim (1999).
6. A. H. Whitehead, J. M. Elliot, and J. R. Owen, *J. Power Sources*, **81-82**, 33 (1999).
7. N. Li and C. Martin, *J. Electrochem. Soc.*, **148**, A164 (2001).
8. Y. Idota, T. Kubota, A. Matsufuji, Y. Maekawa, and T. Misayaka, *Science*, **276**, 1395 (1997).
9. M. Martos, J. Morales, and L. Sánchez, *J. Mater. Chem.*, **12**, 2979 (2002).
10. J. Yang, M. Winter, and J. O. Besenhard, *Solid State Ionics*, **90**, 281 (1996).
11. J. Yang, M. Wachtler, M. Winter, and J. O. Besenhard, *Electrochem. Solid-State Lett.*, **2**, 161 (1999).
12. O. Mao and J. R. Dahn, *J. Electrochem. Soc.*, **146**, 423 (1999).
13. K. D. Kepler, J. T. Vaughey, and M. M. Thackeray, *Electrochem. Solid-State Lett.*, **2**, 307 (1999).
14. J. Fan, T. Wang, C. Yu, B. Tu, Z. Jiang, and D. Zhao, *Adv. Mater. (Weinheim, Ger.)*, **17**, 125 (2005).
15. B. Veeraraghavan, A. Durairajan, B. Haran, B. Popov, and R. Guidotti, *J. Electrochem. Soc.*, **149**, A675 (2002).
16. Y. Wang, J. Y. Lee, and T. C. Deivaraj, *J. Electrochem. Soc.*, **151**, A1804 (2004).
17. C. Nayral, T. Ould-Ely, A. Maisonnat, B. Chaudret, P. Fau, L. Lescouzere, and A. Peyre-Lavigne, *Adv. Mater. (Weinheim, Ger.)*, **11**, 61 (1999).
18. T. Bachels and H. J. Guntherodt, *Phys. Rev. Lett.*, **85**, 1250 (2000).
19. Y. Wang, J. Y. Lee, and B. H. Chen, *J. Electrochem. Soc.*, **151**, A563 (2004).
20. T. P. Kumar, R. Ramesh, Y. Y. Lin, and G. T. Fey, *Electrochem. Commun.* **6**, 520 (2004).
21. Diffraction Data File no. 4-673, ICDD International Center for Diffraction Data (1991).
22. J. Li, H. Li, Z. Wang, L. Chen, and X. Huang, *J. Power Sources*, **107**, 1 (2002).
23. M. Mohamedi, S.-J. Lee, D. Takahashi, M. Nishizawa, T. Itoh, and I. Uchida, *Electrochim. Acta*, **46**, 1161 (2001).
24. M. Wachtler, M. Winter, and J. O. Besenhard, *J. Power Sources*, **105**, 151 (2002).
25. R. Zhang, J. Y. Lee, and Z. L. Liu, *J. Power Sources*, **112**, 596 (2002).